MOLECULAR AND CELLULAR BIOLOGY, Nov. 1995, p. 5879–5887 Vol. 15, No. 11
0270-7306/95/$04.00+0

Endocytosis and Vacuolar Degradation of the Plasma Membrane-Localized Pdr5 ATP-Binding Cassette Multidrug Transporter in *Saccharomyces cerevisiae*

RALF EGNER, YANNICK MAHÉ, RUDY PANDJAITAN, AND KARL KUCHLER*

Department of Molecular Genetics, University and Biocenter of Vienna, A-1030 Vienna, Austria

Received 1 May 1995/Returned for modification 27 June 1995/Accepted 1 August 1995

Multidrug resistance (MDR) to different cytotoxic compounds in the yeast *Saccharomyces cerevisiae* can arise from overexpression of the Pdr5 (Sts1, Ydr1, or Lem1) ATP-binding cassette (ABC) multidrug transporter. We have raised polyclonal antibodies recognizing the yeast Pdr5 ABC transporter to study its biogenesis and to analyze the molecular mechanisms underlying MDR development. Subcellular fractionation and indirect immunofluorescence experiments showed that Pdr5 is localized in the plasma membrane. In addition, pulse-chase radiolabeling of cells and immunoprecipitation indicated that Pdr5 is a short-lived membrane protein with a half-life of about 60 to 90 min. A dramatic metabolic stabilization of Pdr5 was observed in Δ*pep4* mutant cells defective in vacuolar proteinases, and indirect immunofluorescence showed that Pdr5 accumulates in vacuoles of stationary-phase Δ*pep4* mutant cells, demonstrating that Pdr5 turnover requires vacuolar proteolysis. However, Pdr5 turnover does not require a functional proteasome, since the half-life of Pdr5 was unaffected in either *pre1-1* or *pre1-1 pre2-1* mutants defective in the multicatalytic cytoplasmic proteasome that is essential for cytoplasmic protein degradation. Immunofluorescence analysis revealed that vacuolar delivery of Pdr5 is blocked in conditional *end4* endocytosis mutants at the restrictive temperature, showing that endocytosis delivers Pdr5 from the plasma membrane to the vacuole.

An important type of multidrug resistance (MDR) in mammalian tumor cells and cultured cells (19) is caused by gene amplification and subsequent overexpression of the P-glycoprotein (Mdr1) and MDR-associated protein (MRP) (11, 57) transport proteins, both of which are members of the ubiquitous ATP-binding cassette (ABC) protein superfamily (23, 32). P-glycoprotein and MRP are integral plasma membrane proteins that function as ATP-dependent efflux pumps for a variety of structurally unrelated cytotoxic compounds. Elevated P-glycoprotein levels permit tumor cells to survive cytotoxic drug regimens and thus represent a major impediment to curative cancer chemotherapy (9, 19, 57).

The first ABC transporter protein to be identified in the yeast *Saccharomyces cerevisiae* was the Ste6 **a**-factor pheromone transporter (31, 35). Although Ste6 and mammalian P-glycoprotein are structurally closely related, overexpression of Ste6 is not associated with MDR. However, MDR in *S. cerevisiae* is a well-documented phenomenon (33), and there is compelling evidence that MDR in *S. cerevisiae* could be subject to tight transcriptional control by *PDR* (pleiotropic drug resistance) genes encoding transcriptional regulators. For instance, transcription factors such as Pdr1 (2), Yap1/Snq3 (22, 37), Pdr3 (14, 26), and, putatively, Pdr7 and Pdr9 (15) may form a highly complicated network implicated in MDR development (3), similar to P-glycoprotein- or MRP-mediated MDR in mammalian cells. Mutations in *PDR* genes are often associated with MDR, since they are thought to control the expression of individual drug pumps, some of which were shown to be members of the ABC family of multidrug transporters. For example, two highly homologous yeast ABC transporter genes, *SNQ2* (50) and *PDR5*/*STS1*/*YDR1*/*LEM1* (4, 8, 24, 29), hereafter called *PDR5*, were recently shown to represent functional and structural homologs of mammalian Mdr1 because their overexpression in yeast cells is linked to MDR development.

The transcription of *PDR5* is under control of the transcription-regulatory proteins Pdr1 and Pdr3 (14, 26). Genetic experiments have shown that *pdr1*-mediated cycloheximide resistance requires the presence of *PDR5* and that *PDR5* mRNA levels were elevated in a drug-resistant *pdr1-3* mutant (36). By contrast, in Δ*pdr1* Δ*pdr3* double mutants, *PDR5* mRNA synthesis is completely abolished (26). The Pdr5 drug pump was found mainly in membrane preparations enriched for plasma membrane vesicles (4, 13) isolated from *pdr1* mutants, whereas previous studies from crude fractionation experiments of wild-type yeast cells located epitope-tagged Pdr5 to both the plasma membrane and intracellular membranes (8).

Overexpression of *PDR5* and *SNQ2* leads to resistance against a variety of structurally unrelated cytotoxic compounds, including mycotoxins, cycloheximide, staurosporine, cerulenin, 4-nitroquinoline-*N*-oxide, and sulfomethuron methyl (4, 8, 24, 50). However, each transporter mediates resistance to only a distinct subset of drugs (8), and there is very little overlap in the substrate specificity of Pdr5 and Snq2 (24).

The discovery of yeast homologs of mammalian P-glycoproteins suggests the use of *S. cerevisiae* as a paradigm for the study of the molecular mechanisms associated with MDR mediated by ABC transporters. Thus, we have begun to analyze the biogenesis and intracellular trafficking of the yeast Pdr5 drug pump in order to understand the molecular mechanisms underlying MDR development. Here, we report the subcellular localization of the yeast Pdr5 ABC transporter in wild-type cells by refined subcellular fractionation procedures and indirect immunofluorescence. Moreover, by studying the biosynthesis of Pdr5 in mutants lacking cytoplasmic and vacuolar proteinases, we demonstrate that the Pdr5 MDR pump is a rather short-lived protein whose biogenesis involves plasma

* Corresponding author. Mailing address: Department of Molecular Genetics, University and Biocenter of Vienna, Dr. Bohr-Gasse 9/2, A-1030 Vienna, Austria. Phone: 43-1-79515-2111. Fax: 43-1-79515-2900. Electronic mail address: kaku@mol.univie.ac.at.

TABLE 1. Yeast strains used in this study

Strain	Genotype	Reference or Source
YPH500	*MAT*α *ura3-52 his3-Δ200 leu2-Δ1 trp1-Δ63 lys2-801^{amb} ade2-101^{oc}*	8
YKKB-13	*MAT*α *ura3-52 his3-Δ200 leu2-Δ1 trp1-Δ63 lys2-801^{amb} ade2-101^{oc} Δpdr5::TRP1*	8
SF267-1D	*MAT***a** *sec6-4*	R. Schekman
WKK7	*MAT***a** *can1-100 ade2-1^{oc} his3-11,15 leu2-3,112 trp1-1 ura3-1 Δste6::HIS3*	31
VHM3	*MAT***a** *Δste6::HIS3 his3-11,15 ura3-52 leu2-3,112 trp1-1 sec6-4*	This study
YMTAa	*MAT***a** *ura3 his3-11,15 leu2-3,112 Δpep4::HIS3*	D. H. Wolf
WCG4a	*MAT***a** *ura3 his3-11,15 leu2-3,112*	D. H. Wolf
WCG4-11a	*MAT***a** *ura3 his3-11,15 leu2-3,112 pre1-1*	D. H. Wolf
WCG4-11/21a	*MAT***a** *ura3 his3-11,15 leu2-3,112 pre1-1 pre2-1*	D. H. Wolf
RH-268-1C	*MAT***a** *ura3 his4 leu2 bar1-1 end4*	H. Riezman
CB005	*MAT*α *can1-100 ade2-1^{oc} his3-11,15 leu2-3,112 trp1-1 ura3-1 Δpep4::LEU2*	B. Fuller
YAL23	*MAT***a** *ade2-1^{oc} his4 leu2 trp1-1 ura3 Δpep4::LEU2*	This study
YAL24	*MAT***a** *ade2-1^{oc} his3-11,15 leu2 trp1-1 ura3 Δpep4::LEU2 end4*	This study

membrane localization followed by endocytosis and delivery to the vacuole for terminal degradation.

MATERIALS AND METHODS

Media, culture conditions, and strain construction. Rich medium (YPD) and synthetic medium (SD) supplemented with auxotrophic components to maintain plasmids were prepared essentially as described elsewhere (46). All *S. cerevisiae* strains used in this study are listed in Table 1. VHM3, which was kindly provided by V. Huter, is a segregant obtained from a cross between WKK7 and SF267-1D. YAL23 and YAL24 were obtained from a cross between CB005 and RH-268-1C.

Preparation of polyclonal anti-Pdr5 antiserum. Antibodies were raised against a Pdr5-glutathione-*S*-transferase (GST) fusion protein that contains 183 amino acids of the N-terminal part of Pdr5 (amino acids 4 to 187) fused in frame to the C terminus of GST. The gene fusion was constructed by inserting a 555-bp *Sma*I-*Eco*RI fragment of *PDR5*, which was generated by PCR with the custom primers PDR5-GST1 (5′-CAA AAA TGC CCG GGG CCA AGC-3′) and PDR5-GST2 (5′-AAA CGA CTA GGA ATT CAC C-3′), into the *Sma*I and *Eco*RI sites (underlined) of pGEX-3X (Pharmacia), resulting in plasmid pYM21. PCR amplification was performed as described elsewhere (47).

Escherichia coli DH5α carrying pYM21 was grown at 30°C to an optical density at 600 nm (OD_{600}) of 0.7, and expression of the fusion protein was induced by adding isopropyl-β-D-thiogalactopyranoside (IPTG) to a final concentration of 0.1 mM for 4 h. The cells were harvested by centrifugation and resuspended in ice-cold phosphate-buffered saline (PBS) (1/50 of original culture volume). Cell lysis was achieved with a Bandelin Sonopuls HD70 sonicator equipped with an SH70 probe by three 30-s bursts of sonication of the chilled cell suspension at full output. After adding Triton X-100 to a final concentration of 1%, the lysate was centrifuged at 10,000 × *g* to remove insoluble material. The supernatant was incubated with 1 ml of a 50% slurry of glutathione-Sepharose 4B beads (Pharmacia) for 16 h at 4°C on a rotation mixer. The glutathione-Sepharose beads were washed four times with ice-cold PBS, and the fusion protein was eluted by incubating the beads for 10 min with 2 ml of solution of 5 mM reduced glutathione at room temperature. Removal of glutathione and concentration of the Pdr5-GST fusion protein were carried out in a Centricon 10 microconcentrator (Amicon). The purified Pdr5-GST fusion protein was used for immunization of rabbits by standard injection regimens. For immunofluorescence microscopy, the crude rabbit antiserum was affinity purified with the Pdr5-GST fusion protein bound on a nitrocellulose sheet, essentially as described elsewhere (41).

Yeast cell extracts and immunoblotting. Three OD_{600} equivalents of cells were harvested and washed once with H_2O. After repelleting the cells, cell extracts were prepared by lysis with 150 μl of 1.85 M NaOH–7.5% mercaptoethanol for 10 min on ice. Then 150 μl of 50% trichloroacetic acid was added, and the samples were incubated for an additional 10 min on ice. Precipitates were collected by centrifugation at 13,000 × *g* for 3 min. The pellets were dissolved in 50 μl of sample buffer (40 mM Tris-HCl [pH 6.8], 8 M urea, 5% sodium dodecyl sulfate [SDS], 0.1 mM EDTA, 1% mercaptoethanol, 0.01% bromphenol blue) and 10 μl of 1 M Tris base and heated at 42°C for 15 min. Then 20 μl of each sample was electrophoresed through a 7.5% polyacrylamide–SDS gel and transferred to nitrocellulose membranes (BA85; pore size, 0.45 μm; Schleicher & Schüll) as previously described (8). Proteins on immunoblots were visualized with the enhanced chemiluminescence detection system (Amersham) under the conditions recommended by the manufacturer. Antibodies specific for plasma membrane H^+-ATPase (Pma1) were kindly provided by R. Serrano. Antisera against dipeptidylaminopeptidase A (DPAP A) and Sec63 were gifts of T. H. Stevens via R. Kölling and R. Schekman, respectively.

Immunoprecipitation and pulse-chase experiments. Metabolic labeling of yeast cells was performed as described previously (30) with the following modifications. Cells were grown overnight in low-sulfate minimal medium (0.17% yeast nitrogen base without amino acids and without ammonium sulfate [Difco], 2% glucose) supplemented with auxotrophic components and 100 μM ammonium sulfate. Exponentially growing cells (OD_{600}, 0.5 to 1.0) were harvested, resuspended in fresh warmed minimal medium without ammonium sulfate at an OD_{600} of 2, and incubated for 1 h. The cells were metabolically labeled for 30 min by adding 15 μCi of Tran^{35}S-label (ICN Radiochemicals) per OD_{600} unit of cells. An aliquot of 2 OD_{600} units was transferred to a chilled tube, and sodium azide was added to a final concentration of 10 mM. A stock chase solution (100 mM ammonium sulfate, 0.3% L-cysteine, 0.4% L-methionine) was diluted 1:100 into the remaining culture, and samples were removed at intervals. Cells were washed with cold 10 mM sodium azide and resuspended in 200 μl of lysis buffer (50 mM Tris-HCl [pH 7.6], 1 mM EDTA, 1 mM phenylmethylsulfonyl fluoride [PMSF], 10 μg each of chymostatin, leupeptin, antipain, and pepstatin per ml). Lysis was achieved by vigorously vortexing the suspension three times for 1 min each time with glass beads and intermittent cooling for 1 min. After the addition of SDS to 1%, samples were vortexed again twice for 1 min each time. Protein extracts were diluted with 5 volumes of IP buffer (15 mM Tris-HCl [pH 7.5], 150 mM sodium chloride, 1% Triton X-100, 2 mM sodium azide), and the insoluble material was removed by centrifugation. Polyclonal anti-Pdr5 antiserum (10 μl) and 40 μl of a 20% (vol/vol) suspension of protein A-Sepharose beads (Pharmacia) were added to the supernatant and incubated overnight at 4°C on a rotary mixer. Immune complexes bound to the beads were washed three times with IP buffer containing 0.1% SDS and twice with detergent-free wash buffer (10 mM Tris-HCl [pH 7.5], 50 mM sodium chloride, 2 mM sodium azide), resuspended in 45 μl of sample buffer, and heated for 20 min at 42°C. Next, 20 μl of the immunoprecipitated protein, corresponding to 1 OD_{600} unit of cells, was loaded onto a 7.5% polyacrylamide–SDS gel. After electrophoresis, the gel was fixed in 7.5% acetic acid–20% methanol, soaked with En^{3}Hance (NEN DuPont), dried, and exposed to autoradiography film (Fuji RX) at −70°C.

Subcellular fractionation. The procedure for subcellular fractionation of yeast cells is based on sedimentation through sucrose density gradients, as described previously (1). However, to allow clear separation of intracellular organelles, such as the endoplasmic reticulum and Golgi vesicles, from plasma membrane vesicles, the following modifications were developed in this study. Cells were grown in YPD to log phase (OD_{600} of 1). After being chilled on ice, 500 OD_{600} units of cells was harvested by centrifugation at 3,700 × *g* for 10 min. The pellet was resuspended in 30 ml of cold 10 mM sodium azide and centrifuged for 10 min at 500 × *g*. Cells were resuspended to 50 OD_{600} units/ml in spheroplasting buffer (1.4 M sorbitol, 50 mM potassium phosphate [pH 7.5], 10 mM sodium azide, 40 mM mercaptoethanol). Zymolyase 100T (Seikagaku Kogyo Co.) was added to 0.3 mg/ml, and cells were converted to spheroplasts for 30 to 45 min at 30°C with gentle shaking. All further steps were carried out at 0 to 4°C. The spheroplast suspension was chilled on ice and centrifuged at 500 × *g* for 10 min. The pellet was gently resuspended in 10 ml of spheroplasting buffer, recentrifuged once at 500 × *g* for 10 min, and resuspended in 5 ml of lysis buffer (0.8 M sorbitol, 10 mM MOPS [morpholinepropanesulfonic acid, pH 7.2], 1 mM EDTA, 1 mM PMSF). The spheroplasts were lysed with 30 to 60 strokes of a tissue grinder (Kontes Scientific Glassware; pestle B). The lysate was spun for 10 min at 2,000 × *g* to remove unlysed cells and debris, and 2 ml of the resulting supernatant was layered onto a step gradient containing 1 ml each of 12, 18, 24, 30, 36, 42, 48, and 54% (wt/vol) sucrose and a 0.5-ml step of 60% (wt/vol) sucrose in lysis buffer. Gradients were spun for 3 h at 150,000 × *g* (34,000 rpm) in an SW40 Ti rotor (Beckman Instruments) at 4°C. Fractions (1 ml) were harvested bottom to top from the gradients with a low-pressure chromatography pump. The enzyme activities of organelle marker enzymes were determined with 25- or 50-μl aliquots of each fraction. For immunoblot analysis, a 100-μl aliquot of each fraction was concentrated by trichloroacetic acid precipitation and used for SDS-polyacrylamide gel electrophoresis (PAGE) as described above.

For crude subcellular fractionation experiments, cell lysates were prepared as indicated above and subjected to differential centrifugation at 4°C at 10,000 × *g* (13,500 rpm, TLA-100.3 rotor; Beckman Instruments) for 15 min essentially as described previously (8). The supernatant fraction S1 was removed from pellet P1 and centrifuged at 200,000 × *g* (60,000 rpm, TLA-100.3) for 40 min to yield pellet P2 and supernatant S2. Aliquots of each fraction were prepared for SDS-PAGE and immunoblotting as described above. Protein content was determined by the method of Lowry et al. as described previously (30).

Enzyme assays. The reaction mixture to measure NADPH-cytochrome *c* reductase consisted of 0.1% cytochrome *c*, 50 mM potassium phosphate (pH 7.5), 0.4 mM potassium cyanide, 1 μM flavin mononucleotide, 0.1% Triton X-100, and 0.25 mM NADPH. The increase in A_{550} during the reduction of cytochrome *c* was monitored. Vacuolar α-mannosidase was assayed through the generation of *p*-nitrophenol from *p*-nitrophenyl-α-mannoside, which leads to an increase in A_{405}. The reaction mixture consisted of 100 mM MES (morpholineethanesulfonic acid)-NaOH (pH 6.5), 0.2% Triton X-100, and 4 mM *p*-nitrophenyl-α-mannoside. The reaction was stopped by adding 1 volume of 0.5 M sodium carbonate.

Indirect immunofluorescence. Immunofluorescence of yeast cells was carried out essentially as described elsewhere (30) with the following modifications. About 10 OD_{600} units of cells was grown in YPD and fixed by adding formaldehyde directly to the culture to a final concentration of 5% (vol/vol). After 2 h at room temperature or overnight at 30°C in 4% formaldehyde–50 mM magnesium chloride–100 mM potassium phosphate (pH 6.5), if the cells were to be used with Nomarski optics to visualize vacuoles, the cells were recovered by centrifugation and washed in 1 ml of 100 mM Tris-HCl (pH 7.6)–10 mM EDTA. Cells were then incubated for 10 min at room temperature in 600 μl of solution I (0.1 M Tris-H_2SO_4 [pH 9.4], 2% mercaptoethanol) and washed with spheroplasting buffer (0.1 M sodium citrate [pH 7.0], 60 mM EDTA, 1 M sorbitol). Cell walls were removed by incubation of the cells in 1 ml of spheroplasting buffer containing 25 mM mercaptoethanol and 70 μg of Zymolyase 100T per ml for 45 min at 30°C with gentle shaking. Spheroplasts were washed twice with 1 ml of solution II (50 mM Tris-HCl [pH 7.6], 20 mM EDTA, 1.2 M sorbitol) and twice with 1 ml of PBS. Finally, the spheroplasts were suspended to 2 OD_{600} units/ml in PBS.

Multiwell slides (diameter, 7 mm per well) were treated for 30 min with 2% polyethyleneimine and washed with Millipore-filtered water; 30 μl of the spheroplasted cells was applied to each well. After 30 min of incubation, the unbound spheroplasts were aspirated, and the wells were washed six times with PBS. Slides were blocked for 10 min with blocking buffer (PBS, 0.025% Nonidet P-40, 5% bovine serum albumin) prior to antibody decoration for 90 min with affinity-purified anti-Pdr5 antibodies diluted in blocking buffer. Wells were washed 15 times with PBS before incubation with the secondary antibodies (goat anti-rabbit immunoglobulin G [IgG], fluorescein 5-isothiocyanate [FITC] conjugated [Oncogene Science]) diluted in blocking buffer. After 2 h of incubation, the wells were washed 15 times with PBS, stained for 5 min with DAPI (4,6-diamino-2-phenylindole hydrochloride; 1 μg/ml in PBS), washed again six times with PBS, and mounted in Citifluor to minimize photobleaching.

RESULTS

Immunological detection of Pdr5. The *PDR5* DNA sequence predicts an open reading frame of 4,533 bp, encoding a protein of 1,511 amino acids with a calculated molecular mass of 170 kDa (4, 8). To identify the corresponding protein translated from the *PDR5* gene, polyclonal antibodies directed against the N-terminal hydrophilic part (amino acid residues 4 to 187) of the Pdr5 protein were raised in rabbits. Total extracts were prepared from wild-type strain YPH500 and Δ*pdr5* strain YKKB-13 and analyzed by immunoblotting (Fig. 1). A polypeptide band with an apparent molecular mass of 170 kDa was recognized by the antiserum in the wild-type extract, whereas no protein was detectable in the deletion mutant extract. The apparent mobility of authentic Pdr5 in SDS-PAGE gels is in good agreement with the size predicted from the open reading frame contained within the *PDR5* gene and with the size of hemagglutinin epitope-tagged Pdr5 (8).

Pdr5 comigrates with the plasma membrane marker in sucrose velocity gradients. To determine the subcellular localization of Pdr5, cell extracts prepared from gently lysed spheroplasts of strain YPH500 were resolved by velocity sedimentation through sucrose gradients by a modification of a published procedure (1). The modifications of this procedure that we have developed allow for separation of the plasma membrane from intracellular membranes, such as the endoplasmic reticulum, Golgi vesicles, and vacuoles. The subcellular compartments were identified by measuring marker enzyme activities or immunoblotting of proteins typical for a particular organelle (Fig. 2).

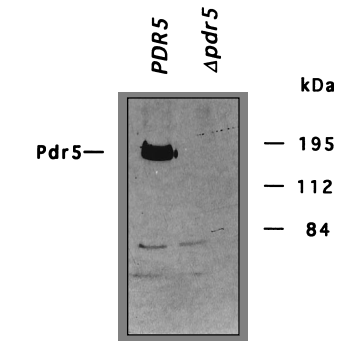

FIG. 1. Immunological detection of Pdr5 protein. Total cell extracts were prepared as described in Materials and Methods. Proteins were separated by SDS-PAGE on a 7.5% gel and analyzed by immunoblotting with antiserum against Pdr5 protein. The lanes contain protein extracts equivalent to 1 OD_{600} unit of cells of wild-type strain YPH500 (*PDR5*) and mutant YKKB-13 (Δ*pdr5*).

The marker enzymes for vacuoles (α-mannosidase), the Golgi vesicles (DPAP A), and the endoplasmic reticulum (Sec63 and NADPH-cytochrome *c* reductase) banded mainly between sucrose concentrations of 30 and 15% (Fig. 2, fractions 6 to 9) but were clearly separated from the plasma membrane marker Pma1, which migrated to a density corresponding to 50 to 40% sucrose (Fig. 2, fractions 3 and 4). The Pdr5 protein

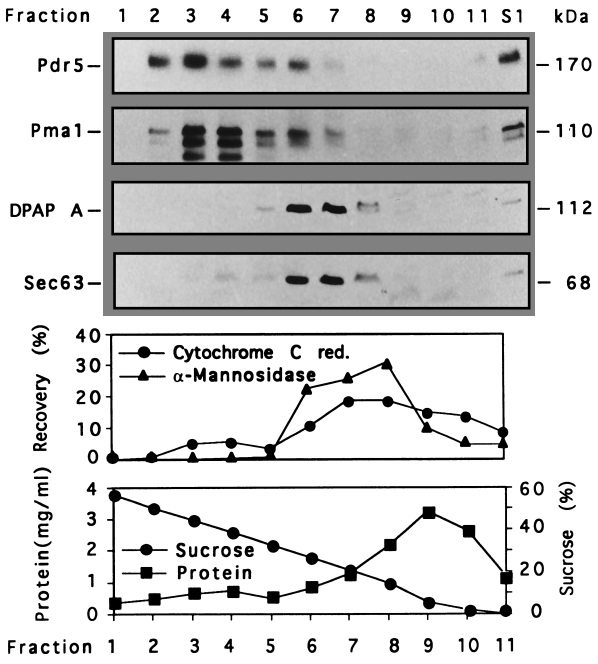

FIG. 2. Subcellular distribution of Pdr5. Pdr5 comigrates with the plasma membrane marker Pma1. The supernatant of a 2,000 × *g* centrifugation step (S1), obtained from a spheroplast lysate of strain YPH500, was layered on a 12 to 60% sucrose gradient. Subcellular organelles were separated during a 3-h spin at 150,000 × *g* as described in Materials and Methods. Aliquots of the gradient fractions were separated on 7.5% polyacrylamide–SDS gels, and the distribution of Pdr5, plasma membrane marker Pma1 (H^+ PM-ATPase), Golgi marker DPAP A, and endoplasmic reticulum marker Sec63 was analyzed by immunoblotting. For enzymatic assays, NADPH-cytochrome *c* reductase was measured as an endoplasmic reticulum marker, and α-mannosidase was used as the vacuole marker. Enzymatic activities are expressed as a percentage of total enzyme activity summed over the whole gradient. Fractions were harvested from the bottom (number 1) to the top (number 11) of the gradient.

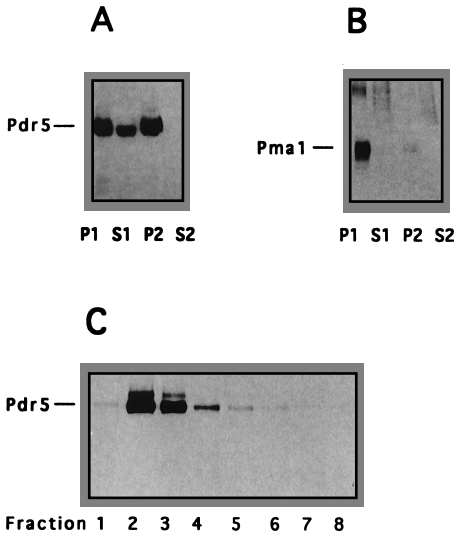

FIG. 3. Distribution of Pdr5 and Pma1 during differential centrifugation of cellular extracts. A total cell extract of strain YMTAa was spun at 10,000 × *g* for 15 min to generate pellet P1. The supernatant S1 was subjected to high-speed centrifugation at 200,000 × *g* for 40 min to yield P2 and S2. Equivalent aliquots of each fraction were analyzed by SDS–7.5% PAGE. Pdr5 and Pma1 were detected on immunoblots with polyclonal antiserum against Pdr5 protein (A) and Pma1 (B). (C) Migration of Pdr5 from the P2 pellet in a sucrose gradient. The P2 pellet obtained from differential centrifugation was layered on a 12 to 60% sucrose step gradient, centrifuged, and fractionated as described in Materials and Methods. Aliquots of fractions were analyzed for Pdr5 by immunoblotting.

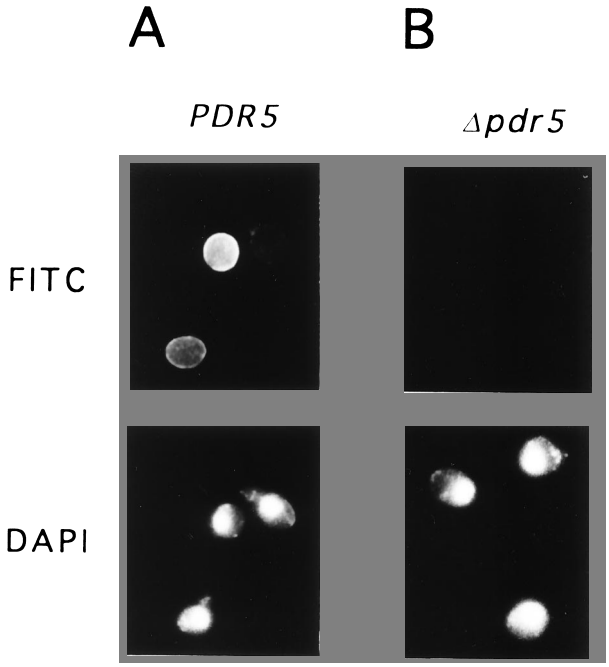

FIG. 4. Pdr5 localizes to the plasma membrane of wild-type cells; indirect immunofluorescence of Pdr5 in wild-type (*PDR5*) (A) and Δ*pdr5* (B) cells. Log-phase wild-type YPH500 (*PDR5*) and mutant YKKB-13 (Δ*pdr5*) cells were fixed and prepared for immunofluorescence as described in Materials and Methods. Cells were treated with affinity-purified anti-Pdr5 antibodies and stained with FITC-conjugated secondary goat anti-rabbit IgG. DNA was visualized with DAPI.

fractionated predominantly with the plasma membrane marker Pma1 and was also clearly separated from the intracellular membrane compartments such as vacuoles, Golgi vesicles, and endoplasmic reticulum (Fig. 2).

The distribution of Pdr5 in cellular membranes was also analyzed by differential centrifugation as described previously (8, 30) (Fig. 3). A cell lysate of strain YMTAa was subjected to centrifugation at 10,000 × *g* to generate pellet P1 and supernatant S1. Subsequent centrifugation of S1 at 200,000 × *g* yielded fractions P2 and S2. The fractions were investigated on immunoblots. The plasma membrane marker Pma1 was found almost exclusively in the P1 pellet (Fig. 3B), and no protein was detectable in the S2 fraction. The Pdr5 protein was found both in P1 and in the high-speed pellet P2 in comparable amounts, and no protein was detectable in the S2 supernatant (Fig. 3A). This distribution is in agreement with the results obtained for epitope-tagged Pdr5 and would also suggest localization in intracellular membranes (8). However, when the high-speed P2 pellet was subjected to further fractionation in the sucrose gradient by velocity sedimentation, the Pdr5 protein was detectable mainly in fractions 2 and 3 (Fig. 3C). This fractionation pattern was very similar to that obtained for Pdr5 and Pma1 when total cell extracts were analyzed in a separate experiment by the standard sucrose gradient fractionation procedure (Fig. 2), suggesting that the immunoreactivity found in P2 is derived from distinct plasma membrane fractions. Indeed, when spheroplasts were treated prior to cell lysis with concanavalin A, a lectin which coats the cell surface, producing sheets of plasma membrane that are readily removed by low-speed centrifugations (38), Pdr5 immunoreactivity was quantitatively recovered during the low-speed 10,000 × *g* centrifugation step, and no Pdr5 protein was detectable in the S1 supernatant, confirming the plasma membrane localization of Pdr5 (data not shown).

Pdr5 is transported to the plasma membrane via the secretory pathway. In another approach to determining the subcellular localization of Pdr5, we used indirect immunofluorescence with affinity-purified polyclonal antibodies against Pdr5 (Fig. 4). Immunofluorescence was carried out with strain YPH500 bearing a chromosomal copy of the *PDR5* gene and its isogenic Δ*pdr5* disruption strain YKKB-13 (8). As is obvious from the bright fluorescence surrounding the cell, the wild-type strain YPH500 gave a predominant rim-like staining pattern typical of plasma membrane proteins (Fig. 4A). As expected, no fluorescence signal could be observed in the Δ*pdr5* control strain YKKB-13 (Fig. 4B), confirming specific recognition of Pdr5 in the plasma membrane of the wild-type strain.

To test whether plasma membrane localization of Pdr5 requires a functional secretory pathway, we performed indirect immunofluorescence on conditional *sec6-4* mutants, defective in the final step of vesicle delivery to the cell surface (48). The shift of *sec6-4* mutants to the nonpermissive temperature blocks exocytotic vesicle fusion with the plasma membrane and leads to massive intracellular accumulation of secretory vesicles (38) containing newly synthesized proteins on the way to the plasma membrane.

Figure 5 shows the distribution of Pdr5 examined by indirect immunofluorescence in the *sec6-4* mutant strain VHM3 at the permissive temperature (25°C) (Fig. 5A) and after the cells were shifted for 2 h to the nonpermissive temperature of 37°C (Fig. 5B). At the permissive temperature, a ring-like plasma membrane staining, identical to the situation found in normal wild-type cells, was visible, indicating the undisturbed delivery of Pdr5 to the plasma membrane (Fig. 5A; compare with Fig. 4A). However, blocking the secretory pathway for 2 h at 37°C resulted in slightly diffuse, predominantly intracellular vesicu-

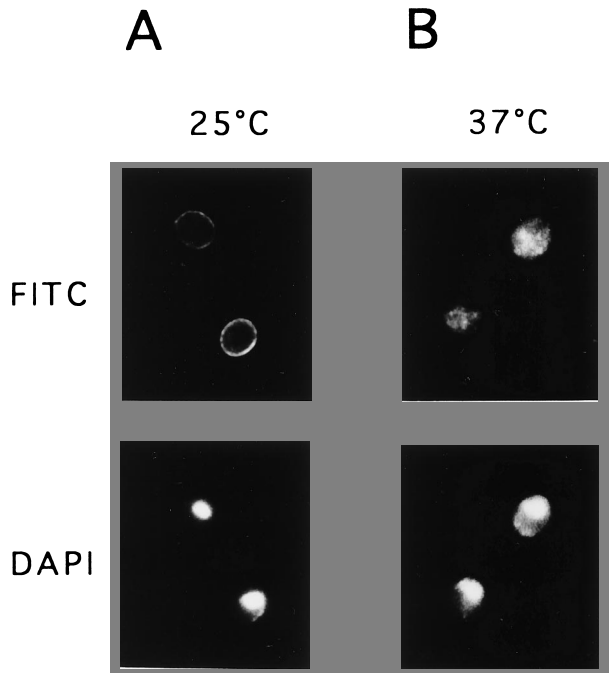

FIG. 5. Indirect immunofluorescence of Pdr5 in late *sec6-4* secretory mutants. The *sec6-4* mutant strain VHM3 (*PDR5*) was grown at 25°C to log phase. Cells were incubated at the permissive temperature (25°C) (A) and for 2 h at the restrictive temperature (37°C) (B), fixed, and prepared for immunofluorescence as described in Materials and Methods. Visualization of Pdr5 localization was performed as described in the legend to Fig. 4.

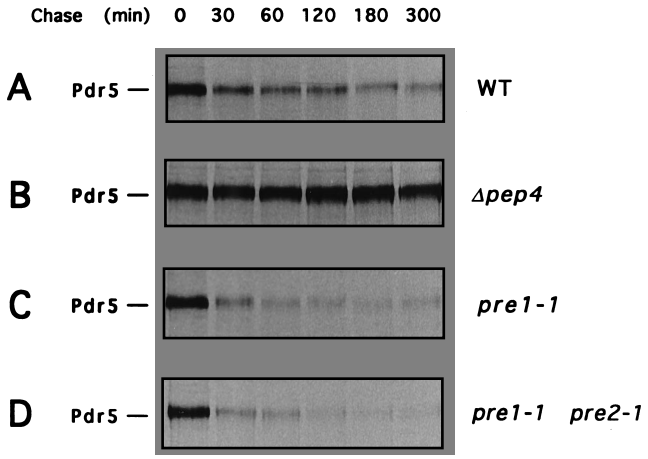

FIG. 6. Pdr5 is stabilized in a Δ*pep4* mutant. Wild-type strain WCG4a (A) and the isogenic proteinase mutants YMTAa (Δ*pep4*) (B), WCG4-11a (*pre1-1*) (C), and WCG4-11/21a (*pre1-1 pre2-1*) (D) were pulse labeled for 30 min and subsequently chased for the times indicated. Aliquots of cell lysates were subjected to immunoprecipitation with anti-Pdr5 antiserum and analyzed by SDS-PAGE and fluorography as described in Materials and Methods.

lar spots and dots like a fluorescence signal, reflecting the accumulation of secretory vesicles with newly synthesized Pdr5 protein destined for the plasma membrane. The corresponding wild-type strain WKK7 showed undisturbed plasma membrane localization of Pdr5 at both 25 and 37°C (data not shown). These findings clearly show that Pdr5 is transported to its destination via the secretory pathway and also confirm the plasma membrane localization of Pdr5.

Turnover of Pdr5 requires vacuolar proteolysis but not the cytoplasmic proteasome. To determine the rate of Pdr5 turnover in the plasma membrane and to determine which proteolytic system is required for Pdr5 turnover, we analyzed the metabolic stability of Pdr5 in yeast cells defective in the two major cellular protein degradation systems. First, the yeast vacuole plays an essential role in the proteolytic turnover of many cellular proteins and is the functional equivalent of the lysosome in mammalian cells (27). In the vacuole, proteinase A is at the top of the hierarchy for the activation of vacuolar hydrolases (55). A lack of proteinase A causes a functional deficiency in several vacuolar proteinases and leads to the accumulation of undegraded cellular proteins (27). The second important cellular protein degradation system, which apparently recognizes ubiquitinated proteins, is represented by the cytoplasmic proteasome, a multienzyme complex consisting of a number of different protease subunits (40). In yeast cells, well-characterized subunits are encoded by the *PRE1* and *PRE2* genes; *pre1-1* and *pre2-2* mutants are severely deficient in cytoplasmic proteolysis and accumulate ubiquitinated proteins (20).

To determine if the vacuole or the proteasome is required for Pdr5 turnover, we analyzed the degradation of Pdr5 at the endpoints of the major cellular degradation pathways. Using pulse-chase experiments, we analyzed the half-life of Pdr5 in the wild-type strain WCG4a and in isogenic strains lacking either proteinase A (Δ*pep4*) or the chymotrypsin-like activity of the proteasome (*pre1-1* and *pre1-1 pre2-1*) (Fig. 6). Yeast cells were metabolically labeled for 30 min with Tran^{35}S-label, and the decrease in radiolabeled Pdr5 was monitored for 5 h. In the wild-type strain WCG4a, the Pdr5 protein was found to be unstable (Fig. 6A), with a half-life of about 60 to 90 min. However, in the Δ*pep4* strain lacking the vacuolar proteinase A, Pdr5 was stable over the chase period of 5 h (Fig. 6B). In contrast, Pdr5 stability was essentially the same in the *pre1-1* (Fig. 6C) and *pre1-1 pre2-1* double (Fig. 6D) mutants as that in the wild-type strain WCG4a (Fig. 6A). These results demonstrate that cellular turnover of Pdr5 mainly depends on vacuolar proteolysis, not on the cytoplasmic proteasome, and imply that Pdr5 is delivered from the plasma membrane to the vacuole for terminal degradation.

Pdr5 accumulates in vacuoles of a Δ*pep4* strain. As demonstrated in Fig. 6, the proteolytic turnover of cellular Pdr5 requires vacuolar proteinases. To directly visualize the arrival and accumulation of Pdr5 in the vacuole, the cellular distribution of Pdr5 was examined by indirect immunofluorescence in Δ*pep4* mutant cells (Fig. 7). The protein degradation rate in the vacuole is low during log phase but increases severalfold when cells enter the stationary phase and under nutritional stress conditions (52). Thus, cells reaching the stationary phase were harvested and prepared for immunofluorescence.

The wild-type strain exhibited the typical rim-staining pattern indicative of plasma membrane localization of Pdr5 (Fig. 4). In contrast, in the Δ*pep4* mutant cells, an intense intracellular fluorescence signal in addition to some residual rim staining showed the accumulation of Pdr5 in the vacuole; Pdr5 could not be significantly degraded because of a severely impaired proteolytic capacity of the vacuoles in the Δ*pep4* mutant (Fig. 7). The use of Nomarski optics, which allowed visualization of the vacuoles, confirmed the overlap of the fluorescence signal from Pdr5 with the vacuoles. By contrast, the wild-type strain showed no vacuolar staining in any growth phase examined, presumably because the active proteolysis of the wild-type vacuole kept the steady-state levels of Pdr5 below the detection limit (data not shown). These results demonstrate that cellular proteolysis of Pdr5 occurs mainly, if not exclu-

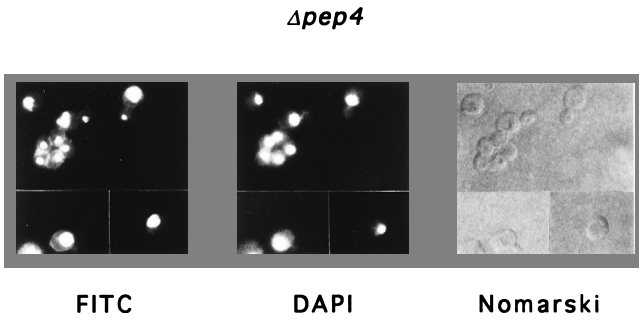

FIG. 7. Pdr5 accumulates in the vacuole of a Δ*pep4* mutant. Cells of the proteinase A mutant YMTAa (Δ*pep4*) were fixed with formaldehyde in the early stationary phase and processed for indirect immunofluorescence as described in Materials and Methods. Cells were stained with anti-Pdr5 antibodies followed by FITC-conjugated goat anti-rabbit IgG (FITC). Visualization of DNA and vacuoles was performed with DAPI and by Nomarski images.

sively, in the vacuole and suggest that the endocytic pathway is required for the delivery of Pdr5 from the plasma membrane to the vacuole.

Endocytosis delivers plasma membrane Pdr5 to the vacuole. To answer whether or not endocytosis is required for vacuolar delivery of Pdr5, we analyzed the fate of Pdr5 in *end4* mutants, in which the initial step of the endocytic pathway, endocytic vesicle formation, is blocked at the restrictive temperature (42). In exponentially grown Δ*pep4* mutants, Pdr5 was found in the plasma membrane and to a certain extent in the vacuoles at both 24 and 37°C, as evident from the rim staining and the amount of immunoreactive material in the vacuole (Fig. 8A). As expected, Pdr5 gave a similar staining pattern at the permissive temperature in the Δ*pep4 end4* double mutant (Fig. 8B). In contrast, however, immunofluorescence of Δ*pep4 end4* double mutants shifted to the restrictive temperature revealed that Pdr5 accumulated on the cell surface and could no longer be delivered to the vacuole (Fig. 8B). In this strain, the vacuole appeared to be devoid of detectable Pdr5 immunoreactive material at 37°C, which was also obvious when the vacuoles of the same cells were visualized by Nomarski optics (Fig. 8B). In addition, the plasma membrane fluorescence signal was much more intense in Δ*pep4 end4* double mutants at the restrictive temperature, suggesting that Pdr5 actually accumulated at the cell surface of endocytosis mutants because it could no longer be delivered to the vacuole (Fig. 8B). Together, these data demonstrate that a functional endocytic pathway is required for delivery of cell surface Pdr5 to the vacuoles.

DISCUSSION

The *PDR5* gene was recently cloned independently in several laboratories by using genetic screens based on the ability of Pdr5 to confer high-copy-mediated resistance to normally cytotoxic concentrations of various drugs (4, 8, 24). In the present study, we used a refined subcellular fractionation procedure and indirect immunofluorescence to show that Pdr5 is localized mainly in the plasma membrane (Fig. 2 and 4). Similarly, Pdr5 was previously found in plasma membrane-enriched membrane vesicle preparations isolated from *pdr1-3* mutants, in which Pdr5 is apparently overexpressed (4). In addition, our results demonstrate that the plasma membrane targeting of Pdr5 requires a functional secretory pathway, as Pdr5 accumulates intracellularly at the restrictive temperature in late secretory mutants, such as *sec6-4* mutants (48, 54) (Fig. 5). Moreover, we have recently found that Pdr5 is a glycosylated protein (17), confirming transport of Pdr5 to the cell surface via the secretory pathway.

The cell surface localization of Pdr5 appears to be only transient, because our results demonstrate that plasma membrane targeting of Pdr5 is followed by its delivery to the vacuole for terminal degradation (Fig. 6 to 8). Similar findings were recently reported for the Fur4 uracil permease, whose degradation is induced under nutritional stress conditions (53), the Ste2/Ste3 mating pheromone receptors (12), and the Ste6 **a**-factor pheromone transporter (6, 28). Except for Fur4, all of these proteins, including Pdr5, appear to be rather short-lived under normal growth conditions, and their delivery to the vacuole occurs via endocytosis, for which at least two different mechanisms seem to exist in *S. cerevisiae* (44). One type of endocytosis occurs constitutively and, as in the case of the pheromone receptors, occurs even in the absence of mating pheromones (12), whereas receptor-mediated endocytosis, the second mechanism, is induced by binding of pheromone ligands to their specific cell surface receptors (12, 45).

While one can predict that most, if not all, cell surface proteins have to undergo endocytosis at some point within their life cycle, this cannot explain the vastly different half-lives of surface proteins. For instance, the half-life of Pma1 exceeds 10 h (5), whereas Ste6 (28) and Pdr5 are rather short-lived, exhibiting half-lives of about 10 and 90 min, respectively. Assuming that all plasma membrane proteins are endocytosed at the same rate, different turnover rates of proteins could then be brought about if long-lived proteins are efficiently recycled to the surface via recycling endosomes (51), whereas short-lived proteins are subject to direct and rapid delivery to the vacuole. Indeed, such a mechanism of protein recycling has been demonstrated to exist in mammalian cells as the principal means for recycling of many different cell surface receptors that efficiently escape lysosomal degradation after endocytosis (10).

In any case, it seems obvious that there must be signals for both recycling and endocytosis of surface proteins. Interestingly, a potential endocytosis signal was recently identified in the Ste2 pheromone receptor in the C-terminal sequence DAKSS (45). Deletion of this motif or a DARSS mutation in an Ste2 variant that is truncated at amino acid 345 leads to a complete lack of regulated Ste2 endocytosis (45). Notably, we have found a somewhat similar sequence in both Pdr5 and Ste6, but it is not known at present if a DAKSS-like motif can also mediate endocytosis of cell surface proteins like Pdr5.

The vacuole is the primary organelle for nonspecific proteolysis in the yeast cell (27). Our results demonstrate that Pdr5 turnover requires a functional endocytic pathway (Fig. 8) and show that Pdr5 degradation occurs mainly in the vacuole, since Pdr5 is stabilized in cells lacking vacuolar proteinase A (Fig. 6B) and because Pdr5 stabilization is accompanied by accumulation of the protein in the vacuole of *pep4* mutant cells (Fig. 7).

The second important cellular protein degradation system in yeast cells is represented by the cytoplasmic proteasome, a multienzyme complex consisting of 14 different subunits (21). Yeast proteasome mutants are unable to degrade short-lived soluble proteins such as metabolically regulated enzymes (49), the *MAT*α2 repressor (43), and proteins required for cell cycle progression, such as Cln3 (56). Proteasome mutants exhibit a severe proteolysis-deficient phenotype, leading to the accumulation of ubiquitinated proteins (20), since ubiquitination of proteins is believed to be the trigger for protein breakdown through the proteasome (25). Interestingly, there is indirect evidence for a function of ubiquitin in membrane protein degradation as well. For instance, the Fur4 uracil permease is

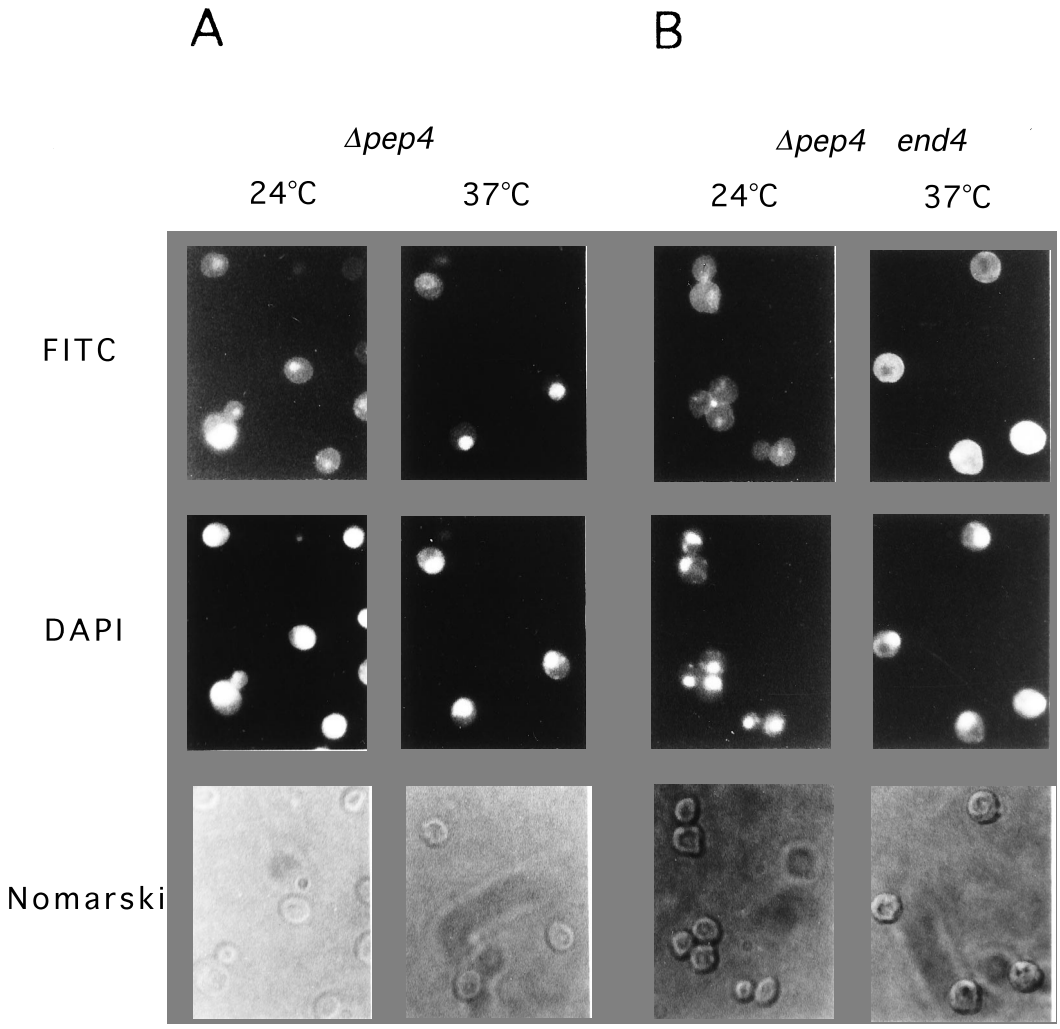

FIG. 8. Pdr5 accumulates at the cell surface of *end4* endocytosis mutants. The isogenic strains YAL23 (Δ*pep4*) (A) and YAL24 (Δ*pep4 end4*) (B) were grown at 25°C and shifted to the nonpermissive temperature of 37°C for 2 h before being fixed with formaldehyde. Cells were prepared for immunofluorescence analysis as described in Materials and Methods. Cells were stained with anti-Pdr5 antibodies followed by FITC-conjugated goat anti-rabbit IgG (FITC). Visualization of DNA was performed with DAPI. Exposure times: (A) YAL23, 1 s each at 24 and 37°C; (B) YAL24, 1 and 0.5 s at 24 and 37°C, respectively.

stabilized against degradation by a point mutation in a cyclin-like "destruction box" under nutritional stress conditions (18), and Ste6 is ubiquitinated prior to endocytosis (28). While a functional role for the proteasome in Fur4 or Ste6 turnover was not shown (28, 53), our results demonstrate that the cytoplasmic proteasome is not involved in Pdr5 turnover, because Pdr5 stability is not increased in the proteasomal *pre1-1* and *pre1-1 pre2-1* mutants (Fig. 6). Thus, turnover of Ste6 and Pdr5, both of which are ubiquitinated in vivo (16, 28), requires a functional vacuole but not the cytoplasmic proteasome. Whether or not ubiquitination of cell surface proteins such as Ste6 and Pdr5 can function as a signal for endocytosis and/or delivery to the vacuole remains to be established in future studies.

It seems reasonable that the Pdr5 MDR transporter actually has to undergo constitutive endocytosis. For instance, various transporters for different nutrients and/or carbon sources may not be required at all times during cellular growth. By the same token, MDR transporters such as Pdr5 and its close homolog Snq2 (50) may not always be required for cellular detoxification and are therefore constantly removed from the surface. However, when needed, their expression can be efficiently induced to satisfy an increased requirement for an active transporter. Indeed, expression of both Pdr5 and Snq2 is dramatically increased in *pdr1* mutants that exhibit a pleiotropic MDR phenotype (34). A possible function for the Pdr5 and Snq2 transporters in detoxification is further supported by the fact that the biogenesis and turnover of Pdr5 involve both the exocytic and endocytic pathways. Thus, Pdr5 could mediate extrusion of toxic metabolites at three levels: (i) within the secretory pathway en route to the cell surface; (ii) from the cytoplasm across the plasma membrane; and (iii) during endocytic transport to the vacuole. Such a system would be very effective indeed, and given that it could comprise several transporters with different substrate specificities, such as Pdr5 and Snq2, it could handle a variety of toxic challenges to the cell. Remarkably, we have identified at least two additional yeast ABC transporter genes (7) closely related to *PDR5* and *SNQ2*, one of which is most likely to be *PDR10*, recently identified on chromosome XV during the course of the yeast genome sequencing (39). Thus, the construction of triple and eventually quadruple deletion mutants of the small gene family encoding

novel multidrug ABC transporters closely related to Pdr5 will shed light on their putative function in cellular detoxification or help to uncover the elusive physiological functions of Pdr5 and its homologs.

ACKNOWLEDGMENTS

We are greatly indebted to R. Kölling, H. Riezman, R. Serrano, R. Schekman, B. Fuller, T. Stevens, and D. H. Wolf for generously providing yeast strains, antibodies, and reagents. Thanks to A. Parle and K. Wolfe for sharing unpublished results. The critical and helpful comments on the manuscript by D. Marks and A. Parle and the expert tetrad dissecting skills of A. Lamprecht are thankfully acknowledged. We thank R. Kukina for her patience in doing the artwork.

The work carried out in this study was supported by a grant from the Austrian Science Foundation (P-10123). Y.M. and R.P. were supported in part by funds from the Austrian National Bank (project 4486) and by the Commission of Oncology of the University of Vienna, respectively. R.E. was supported in part by a postdoctoral fellowship from the Deutsche Forschungsgemeinschaft.

REFERENCES

1. **Antebi, A., and G. R. Fink.** 1992. The yeast Ca(2+)-ATPase homologue, *PMR1*, is required for normal Golgi function and localizes in a novel Golgi-like distribution. Mol. Biol. Cell **3:**633–654.
2. **Balzi, E., W. Chen, S. Ulaszewski, E. Capieaux, and A. Goffeau.** 1987. The multidrug resistance gene *PDR1* from *Saccharomyces cerevisiae*. J. Biol. Chem. **262:**16871–16879.
3. **Balzi, E., and A. Goffeau.** 1994. Genetics and biochemistry of yeast multidrug resistance. Biochim. Biophys. Acta **1187:**152–162.
4. **Balzi, E., M. Wang, S. Leterme, L. Van Dyck, and A. Goffeau.** 1994. *PDR5*, a novel yeast multidrug resistance conferring transporter controlled by the transcription regulator *PDR1*. J. Biol. Chem. **269:**2206–2214.
5. **Benito, B., E. Moreno, and R. Losario.** 1991. Half-life of plasma membrane ATPase and its activating system in resting yeast cells. Biochim. Biophys. Acta **1063:**265–268.
6. **Berkower, C., D. Loayza, and S. Michaelis.** 1994. Metabolic instability and constitutive endocytosis of *STE6*, the **a**-factor transporter of *Saccharomyces cerevisiae*. Mol. Biol. Cell **5:**1185–1198.
7. **Bissinger, P. H., and K. Kuchler.** Unpublished data.
8. **Bissinger, P. H., and K. Kuchler.** 1994. Molecular cloning and expression of the *Saccharomyces cerevisiae STS1* gene product: a yeast ABC transporter conferring mycotoxin resistance. J. Biol. Chem. **269:**4180–4186.
9. **Borst, P., A. H. Schinkel, J. J. Smit, E. Wagenaar, L. Van Deemter, A. J. Smith, E. W. Eijdems, F. Baas, and G. J. Zaman.** 1993. Classical and novel forms of multidrug resistance and the physiological functions of P-glycoproteins in mammals. Pharmacol. Ther. **60:**289–299.
10. **Brown, V. I., and M. I. Greene.** 1991. Molecular and cellular mechanisms of receptor mediated endocytosis. DNA Cell Biol. **10:**309–409.
11. **Cole, S. P., G. Bhardwaj, J. H. Gerlach, J. E. Mackie, C. E. Grant, K. C. Almquist, A. J. Stewart, E. U. Kurz, A. M. Duncan, and R. G. Deeley.** 1992. Overexpression of a transporter gene in a multidrug-resistant human lung cancer cell line. Science **258:**1650–1654.
12. **Davis, N. G., J. L. Horecka, and G. F. Sprague.** 1993. *Cis-* and *trans*-acting functions required for endocytosis of the yeast pheromone receptors. J. Cell Biol. **122:**53–65.
13. **Decottignies, A., M. Kolaczkowski, E. Balzi, and A. Goffeau.** 1994. Solubilization and characterization of the overexpressed *PDR5* multidrug resistance nucleotide triphosphatase of yeast. J. Biol. Chem. **269:**12797–12803.
14. **Delahodde, A., T. Delaveau, and C. Jacq.** 1995. Positive autoregulation of the yeast transcription factor Pdr3p, which is involved in control of drug resistance. Mol. Cell. Biol. **15:**4043–4051.
15. **Dexter, D., W. S. Moye-Rowley, A. L. Wu, and J. Golin.** 1994. Mutations in the yeast *PDR3*, *PDR4*, *PDR7*, and *PDR9* pleiotropic (multiple) drug resistance loci affect the transcript level of an ATP binding cassette transporter encoding gene, *PDR5*. Genetics **136:**505–515.
16. **Egner, R., and K. Kuchler.** The yeast multidrug transporter Pdr5 of the plasma membrane is ubiquitinated prior to endocytosis and degradation in the vacuole. Submitted for publication.
17. **Egner, R., and K. Kuchler.** Unpublished data.
18. **Galan, J. M., C. Volland, D. Urban-Grimal, and R. Haguenauer-Tsapis.** 1994. The yeast plasma membrane uracil permease is stabilized against stress induced degradation by a point mutation in a cyclin-like "destruction box". Biochem. Biophys. Res. Commun. **201:**769–775.
19. **Gottesman, M., and I. Pastan.** 1993. Biochemistry of multidrug resistance mediated by the multidrug transporter. Annu. Rev. Biochem. **62:**385–427.
20. **Heinemeyer, W., A. Gruhler, V. Möhrle, Y. Mahé, and D. H. Wolf.** 1993. *PRE2*, highly homologous to the human major histocompatibility complex-linked *RING10* gene, codes for a yeast proteasome subunit necessary for chymotryptic activity and degradation of ubiquitinated proteins. J. Biol. Chem. **268:**5115–5120.
21. **Heinemeyer, W., N. Tröndle, G. Albrecht, and D. H. Wolf.** 1994. *PRE5* and *PRE6*, the last missing genes encoding 20S proteasome subunits from yeast? Indication for a set of 14 different subunits in the eukaryotic proteasome core. Biochemistry **33:**12229–12237.
22. **Hertle, K., E. Haase, and M. Brendel.** 1991. The *SNQ3* gene of *Saccharomyces cerevisiae* confers hyper-resistance to several functionally unrelated chemicals. Curr. Genet. **19:**429–433.
23. **Higgins, C. F.** 1992. ABC-transporters: from microorganisms to man. Annu. Rev. Cell Biol. **8:**67–113.
24. **Hirata, D., K. Yano, K. Miyahara, and T. Miyakawa.** 1994. *Saccharomyces cerevisiae YDR1*, which encodes a member of the ATP-binding cassette (ABC) superfamily, is required for multidrug resistance. Curr. Genet. **26:** 285–294.
25. **Jentsch, S.** 1992. The ubiquitin-conjugation system. Annu. Rev. Biochem. **26:**177–205.
26. **Katzmann, D. J., P. E. Burnett, J. Golin, Y. Mahé, and W. S. Moye-Rowley.** 1994. Transcriptional control of the yeast *PDR5* gene by the *PDR3* gene product. Mol. Cell. Biol. **14:**4653–4661.
27. **Knop, M., H. H. Schiffer, S. Rupp, and D. H. Wolf.** 1993. Vacuolar/lysosomal proteolysis: proteases, substrates, mechanisms. Curr. Opin. Cell Biol. **5:**990–996.
28. **Kölling, R., and C. P. Hollenberg.** 1994. The ABC-transporter Ste6 accumulates in the plasma membrane in a ubiquitinated form in endocytosis mutants. EMBO J. **13:**3261–3271.
29. **Kralli, A., S. P. Bohen, and K. R. Yamamoto.** 1995. *LEM1*, an ATP-binding cassette transporter, selectively modulates the biological potency of steroid hormones. Proc. Natl. Acad. Sci. USA **92:**4701–4705.
30. **Kuchler, K., H. Dohlman, and J. Thorner.** 1993. The **a**-factor transporter (*STE6* gene product) and cell polarity in *Saccharomyces cerevisiae*. J. Cell Biol. **120:**1203–1215.
31. **Kuchler, K., R. S. Sterne, and J. Thorner.** 1989. *Saccharomyces cerevisiae STE6* gene product: a novel pathway for protein export in eukaryotic cells. EMBO J. **8:**3973–3984.
32. **Kuchler, K., and J. Thorner.** 1992. Secretion of peptides and proteins lacking hydrophobic signal sequences: the role of ATP-driven membrane translocators. Endocrine Rev. **13:**499–514.
33. **Leppert, G., R. McDevitt, S. C. Falco, T. K. Van Dyk, M. B. Ficke, and J. Golin.** 1990. Cloning by gene amplification of two loci conferring multiple drug resistance in *Saccharomyces*. Genetics **125:**13–20.
34. **Mahé, Y., A. Lamprecht, and K. Kuchler.** The ATP binding cassette multidrug transporter Snq2 of *Saccharomyces cerevisiae*: a novel target for the transcription factor Pdr1. Submitted for publication.
35. **McGrath, J. P., and A. Varshavsky.** 1989. The yeast *STE6* gene encodes a homologue of the mammalian multidrug resistance P-glycoprotein. Nature (London) **340:**400–404.
36. **Meyers, S., W. Schauer, E. Balzi, M. Wagner, A. Goffeau, and J. Golin.** 1992. Interaction of the yeast pleiotropic drug resistance genes *PDR1* and *PDR5*. Curr. Genet. **21:**431–436.
37. **Moye-Rowley, W. S., K. D. Harsham, and C. S. Parker.** 1989. Yeast *YAP1* encodes a novel form of the *jun* family of transcriptional activator proteins. Genes Dev. **3:**283–292.
38. **Nakamoto, R. K., R. Rao, and C. W. Slayman.** 1991. Expression of the yeast plasma membrane $[H^+]$ATPase in secretory vesicles: a new strategy for directed mutagenesis. J. Biol. Chem. **266:**7940–7949.
39. **Parle, A. G., N. J. Hand, S. E. Goulding, and K. Wolfe.** Personal communication.
40. **Peters, J. M.** 1994. Proteasomes: protein degradation machines of the cell. Trends Biochem. Sci. **19:**377–382.
41. **Pringle, J. R., A. E. M. Adams, D. G. Drubin, and B. K. Haarer.** 1991. Immunofluorescence methods for yeast. Methods Enzymol. **194:**565–602.
42. **Raths, S., J. Rohrer, F. Crausaz, and H. Riezman.** 1993. *end3* and *end4*: two mutants defective in receptor-mediated and fluid-phase endocytosis in *Saccharomyces cerevisiae*. J. Cell Biol. **120:**55–65.
43. **Richter-Ruoff, B., D. H. Wolf, and M. Hochstrasser.** 1994. Degradation of the yeast *MAT*α2 transcriptional regulator is mediated by the proteasome. FEBS Lett. **354:**50–52.
44. **Riezman, H.** 1993. Yeast endocytosis. Trends Cell Biol. **3:**273–277.
45. **Rohrer, J., H. Benedetti, B. Zanolari, and H. Riezman.** 1993. Identification of a novel sequence mediating regulated endocytosis of the G protein-coupled α-pheromone receptor in yeast. Mol. Biol. Cell **4:**511–521.
46. **Rose, M. D., F. Winston, and P. Hieter.** 1990. Methods in yeast genetics: a laboratory course manual. Cold Spring Harbor Laboratory Press, Cold Spring Harbor, N.Y.
47. **Sathe, G. M., S. O'Brien, M. M. McLaughlin, F. Watson, and G. P. Livi.** 1991. Use of polymerase chain reaction for rapid detection of gene insertions in whole yeast cells. Nucleic Acids Res. **19:**4775–4781.
48. **Schekman, R.** 1992. Genetic and biochemical analysis of vesicular traffic in yeast. Curr. Opin. Cell Biol. **4:**587–592.
49. **Schork, S. M., G. Bee, M. Thumm, and D. H. Wolf.** 1994. Catabolite inactivation of fructose-1,6-bisphosphatase in yeast is mediated by the pro-

teasome. FEBS Lett. **349:**270–274.
50. **Servos, J., E. Haase, and M. Brendel.** 1993. Gene *SNQ2* of *Saccharomyces cerevisiae*, which confers resistance to 4-nitroquinoline-*N*-oxide and other chemicals, encodes a 169 kDa protein homologous to ATP-dependent permeases. Mol. Gen. Genet. **236:**214–218.
51. **Singer-Krüger, B., R. Frank, F. Crausaz, and H. Riezman.** 1993. Partial purification and characterization of early and late endosomes from yeast: identification of four novel proteins. J. Biol. Chem. **268:**14376–14386.
52. **Teichert, U., B. Mechler, H. Müller, and D. H. Wolf.** 1989. Lysosomal (vacuolar) proteinases of yeast are essential catalysts for protein degradation, differentiation, and cell survival. J. Biol. Chem. **264:**16037–16045.
53. **Volland, C., D. Urban-Grimal, G. Geraud, and R. Haguenauer-Tsapis.** 1994. Endocytosis and degradation of the yeast uracil permease under adverse conditions. J. Biol. Chem. **269:**9833–9841.
54. **Walworth, N. C., and P. J. Novick.** 1987. Purification and characterisation of constitutive secretory vesicles from yeast. J. Cell Biol. **105:**163–174.
55. **Woolford, C. A., J. A. Noble, J. D. Garman, M. F. Tam, M. A. Innis, and E. W. Jones.** 1993. Phenotypic analysis of proteinase A mutants: implications for autoactivation and the maturation pathway of the vacuolar hydrolases of *Saccharomyces cerevisiae*. J. Biol. Chem. **268:**8990–8998.
56. **Yaglom, J., M. H. K. Linskens, S. Sadis, D. M. Rubin, B. Futcher, and D. Finley.** 1995. $p34^{Cdc28}$-mediated control of Cln3 cyclin degradation. Mol. Cell. Biol. **15:**731–741.
57. **Zaman, G. J., M. J. Flens, M. R. Van Leusden, M. de Haas, H. S. Mulder, J. Lankelma, H. M. Pinedo, R. J. Scheper, F. Baas, H. J. Broxterman, and P. Borst.** 1994. The human multidrug resistance-associated protein MRP is a plasma membrane drug-efflux pump. Proc. Natl. Acad. Sci. USA **91:**8822–8826.